Journal of
PERIODONTAL RESEARCH

J Periodont Res 2011; 46: 228–234

JOURNAL OF PERIODONTAL RESEARCH
doi:10.1111/j.1600-0765.2010.01334.x

Photobleaching of red fluorescence in oral biofilms

C. K. Hope[1], E. de Josselin de Jong[1,2], M. R. T. Field[3], S. P. Valappil[1], S. M. Higham[1]

[1]School of Dental Sciences, University of Liverpool, Liverpool, UK, [2]Inspektor Research Systems BV, Amsterdam, The Netherlands and [3]Department of Human Anatomy and Cell Biology, University of Liverpool, Liverpool, UK

Hope CK, de Josselin de Jong E, Field MRT, Valappil SP, Higham SM. Photobleaching of red fluorescence in oral biofilms. J Periodont Res 2011; 46: 228–234. © 2010 John Wiley & Sons A/S

Background and Objective: Many species of oral bacteria can be induced to fluoresce due to the presence of endogenous porphyrins, a phenomenon that can be utilized to visualize and quantify dental plaque in the laboratory or clinical setting. However, an inevitable consequence of fluorescence is photobleaching, and the effects of this on longitudinal, quantitative analysis of dental plaque have yet to be ascertained.

Material and Methods: Filter membrane biofilms were grown from salivary inocula or single species (*Prevotella nigrescens* and *Prevotella intermedia*). The mature biofilms were then examined in a custom-made lighting rig comprising 405 nm light-emitting diodes capable of delivering 220 W/m^2 at the sample, an appropriate filter and a digital camera; a set-up analogous to quantitative light-induced fluorescence digital. Longitudinal sets of images were captured and processed to assess the degradation in red fluorescence over time.

Results: Photobleaching was observed in all instances. The highest rates of photobleaching were observed immediately after initiation of illumination, specifically during the first minute. Relative rates of photobleaching during the first minute of exposure were 19.17, 13.72 and 3.43 arbitrary units/min for *P. nigrescens* biofilms, microcosm biofilm and *P. intermedia* biofilms, respectively.

Conclusion: Photobleaching could be problematic when making quantitative measurements of porphyrin fluorescence *in situ*. Reducing both light levels and exposure time, in combination with increased camera sensitivity, should be the default approach when undertaking analyses by quantitative light-induced fluorescence digital.

Chris Hope, BSc(Hons.), PhD, FHEA, School of Dental Sciences, University of Liverpool, Research Wing, Daulby Street, Liverpool L69 3GN, UK
Tel: +44 0 151 706 5296
Fax: +44 0 151 706 5809
e-mail: chope@liv.ac.uk

Key words: oral biofilm; plaque; fluorescence; quantitative light-induced fluorescence digital; porphyrin; photobleaching

Accepted for publication November 4, 2010

Fluorescentporphyrins are present in many members of our indigenous microbiota (1,2), including those found in the oral cavity (3–5). Whilst many bacterial porphyrins are associated with photosynthesis, a relatively large amount of haem (iron protoporphyrin IX), for example, is incorporated on the cell surface of the putative periodontal pathogen *Porphyromonas gingivalis* to protect it from hydrogen peroxide (6), with similar processes occurring in *Prevotella nigrescens* and *Prevotella intermedia* (7; both formerly classified as *Bacteroides melanogenicus*; 8). The molecular fluorescence of bacterial porphyrins is an adventitious phenomenon, which results from the absorption of a photon and the subsequent re-emission of another photon of a longer wavelength as the electrons in the molecule return from the excited (triplet) state to the ground state. Specific porphyrins have distinct excitation spectra with different maxima; protoporphyrin at 593 nm and coproporphyrin at 604 nm (9). The wavelengths suitable for the efficient fluorescent excitation of bacterial porphyrins range from near ultraviolet (300 nm) to blue (450 nm). The discrepancy between the colour of the incident light and the fluorescent emission, a phenomenon known as the Stokes shift (10), allows for the selective capture and quantification of the emitted light via an appropriate filter set-up.

Photobleaching occurs when a fluorophore is irreversibly damaged so that it no longer fluoresces. Although the exact mechanisms by which

photobleaching occur are not clear, it has been suggested that the fluorophores undergo an oxidative reaction with highly reactive oxygen species such as singlet oxygen ($^1O_2$) and hydroxyl radicals ($OH^{\cdot}$; 11). Molecules already in the excited (singlet) state can also be destructively excited by an additional excitation photon, an event dubbed two-photon excitation, but it is unlikely that this process would occur in the experiments discussed herein. Other results have demonstrated photobleaching reactions occurring between excited dye molecules (12). The generation of highly reactive oxygen species has also been demonstrated to cause cell death in *P. gingivalis*, *P. nigrescens* and *P. intermedia* by the excitation of endogenous porphyrins (13). Lethal photosensitization (photodynamic therapy), either by the application of photosensitizing agents or via endogenous porphyrins, has the potential to be an effective means of treating plaque-related diseases (14).

Fluorescence microscopy techniques can utilize the kinetics of photobleaching by fluorescence loss in photobleaching (FLIP) and fluorescence recovery after photobleaching (FRAP) to reveal rates of diffusion within cell membranes, organelles (15) and biofilms (16). However, when undertaking quantitative measurements of fluorescence, photobleaching can be problematic (17).

Quantitative light-induced fluorescence (QLF) uses violet light to induce fluorescence in tooth enamel and collects the resulting emissions via a high band-pass filter (>520 nm) in conjunction with a computer-controlled digital camera (18). When viewed under QLF lighting conditions, areas of demineralized enamel fluoresce less than surrounding sound enamel and so appear darker. Regions of demineralized enamel are visible under QLF lighting conditions before they are visible to the eye as white spot lesions (19). Although QLF was initially developed for the analysis of tooth enamel (20), it has been subsequently demonstrated to be capable of revealing dental plaque due to the fluorescence of endogenous porphyrins (5). However, since the filter configuration of QLF was designed to maximize the transmission of green light, there are limitations as to its usefulness for the analysis of dental plaque (21). Quantitative light-induced fluorescence digital (QLFD) is an adaptation of QLF which employs a modified filter set (D007; Inspektor Research Systems BV, Amsterdam, The Netherlands), narrow-band violet light (405 nm) and a high-specification digital single-lens reflex (SLR) camera. This configuration has been specifically developed to enhance the visualization and quantification of plaque. During clinical investigations to assess plaque, QLFD is typically used to identify regions of red fluorescence and capture a sequence of images at different visits in order to quantify the progression of conservative dental treatment.

A better understanding of photobleaching phenomena with respect to indigenous bacterial porphyrins, illuminated by QLFD lighting, *in situ* is required to enable accurate quantitative analyses of dental plaque to be undertaken.

Material and methods

Filter membrane biofilms

Approximately 10 mL of unstimulated saliva was obtained from a healthy volunteer with no previous history of periodontitis. This was split into 1 mL aliquots and frozen. Nitrocellulose filter membranes (47 mm diameter, 0.45 μm pore size; Invitrogen Ltd, Paisley, Renfrewshire, UK) were laid, with their inked grid upwards, on top of blood agar (Oxoid, Basingstoke, UK) supplemented with 5% defibrinated horse blood. A 50 μL aliquot of the saliva sample was spread over the membrane before being incubated at 37°C in anaerobic conditions (80% N_2, 10% CO_2, 10% H_2) for 7 d to allow microcosm oral biofilms to develop. Individual biofilm-laden filter membranes were removed from the supporting agar and placed in a Petri dish, which had first had 200 μL of phosphate-buffered saline beaded over the surface to help prevent the membrane biofilm from drying out. Similar single-species biofilms were grown using heavy colony inocula of *Prevotella nigrescens* (ATCC 25261; 7-d-old cultures) or *Prevotella intermedia* (ATCC 25611; 5-d-old cultures) suspended in 1 mL of phosphate-buffered saline.

Fluorescence imaging

A custom-made rig, incorporating QLFD technology, was constructed to enable the capture of fluorescent images under reproducible lighting conditions from surface-mounted indium gallium nitride light-emitting diodes (LEDs; EWC 400 SC2C, radiant power 600 mW, 23° beam angle; E Wave Corp., London, UK) with a wavelength band from 400 nm to a peak output at 405 nm (violet). To construct the QLFD *in vitro* rig, an LED was soldered onto the outside of a copper ring, being a section of standard domestic plumbing material, which acted as a heat-sink to prevent overheating. Three such mounted LEDs were then fixed inside an approximately hemispherical plastic bowl so that the light beams converged on the sample (Fig. 1). A hole was cut into the base for the unimpeded viewing of the sample by a camera, with another hole in the side-wall to allow the sample to be easily manipulated. The LEDs were powered by a DC adaptor with an output of 5 V at 1.2 A connected in parallel. The distance between the LEDs and the sample was 100 mm at an angle of incidence between camera and LEDs of 30° from the surface normal. The light incident on the sample was measured as irradiance by a photosynthetically active radiometer (PAR) with a cosine corrected detector (Q201 PAR with SD221Q Cos detector; Macam Photometrics Ltd, Livingston, West Lothian, UK). A cut-off filter (D007; Inspektor Research Systems BV) was placed in front of the camera lens to minimize the transmission of light close to the excitation wavelength whilst maximizing the transmission of the red part of the spectrum. All illumination/photobleaching experiments were undertaken in a dark-room.

Images were captured with a 'live view'-enabled digital SLR camera (model 1000D; Canon, Tokyo, Japan)

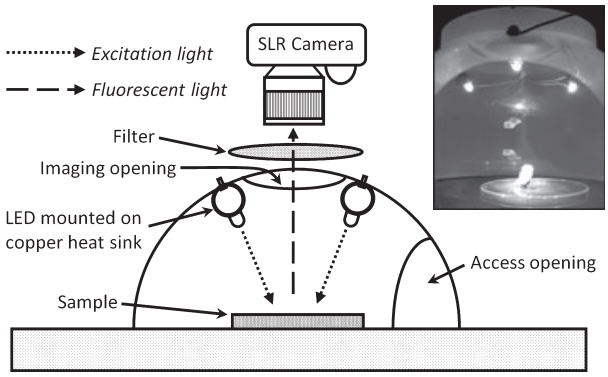

Fig. 1. Schematic diagram of the 405 nm lighting rig, comprising three equidistant indium gallium nitride light-emitting diodes. Inset shows a tooth sample illuminated by the lighting rig.

equipped with a 60 mm, *f*/2.8 macro lens (model: EF-S; Canon) connected to a computer. Proprietary software (C2 v1.0.0.7, Inspektor Research Systems BV) was used to control the camera and store the images. Low apertures (i.e. *f*/2.8 to *f*/8) and ISO settings of 200–400 were typically used to maximize the light sensitivity of the camera without adversely affecting image quality. The camera's on-board 'custom white balance' feature was calibrated against a sheet of white paper before fluorescence imaging to effectively eliminate the colouration of the filter in the resulting images. The camera resolution was set to 'low' (3.4 megapixels) to facilitate the processing of large numbers of data files in the form of uncompressed 24-bit bitmap files. The LEDs were switched on for at least 10 min prior to use to allow their temperature to stabilize. Without moving the sample or changing camera settings, a series of images was captured over time using the in-built image sequencer incorporated into the control software. Control experiments included membranes that were partly covered with aluminium foil to shield portions of them from the light. Four separate microcosm biofilm photobleaching experiments were undertaken, whilst the experiments for single species were conducted in duplicate.

Image analysis

Images were analysed with an open-source software package (ImageJ 1.43q; The National Institutes of Health, Bethesda, MD, USA, http://rsb.info.nih.gov/ij/). The images comprising the time-lapse sequence were opened with ImageJ and compiled into a single image 'stack'. The stack was then split into its red, green and blue (RGB) component colour channels; to isolate the red channel as an 8-bit greyscale (i.e. pixel brightness values from 0 to 255). A user-defined 'rectangular selection' region of interest (ROI) was created within one of the inked grid squares on the filter membrane. The size of the grid squares was 4 mm × 4 mm and the ROI encompassed approximately 20,000 pixels. The '*z*-axis profile' of the ROI was then measured through the image stack, and the mean pixel brightness values at each time point were copied into Microsoft Excel. The ROI was then moved to an adjacent square on the grid and the process repeated to give a total of eight discrete counts from the same biofilm sample. The mean pixel brightness values from the eight sample sites were then themselves averaged before being normalized to 100 at time zero to yield the arbitrary unit used throughout these experiments, 'normalized mean pixel brightness' (NMPB), which allowed the direct comparisons to be made between separate experiments.

Changes in fluorescence (ΔF) were calculated in terms of the shift in NMPB per unit time to yield results in terms of ΔF per minute. These ΔF values were then allocated into subsets to determine mean ΔF between discrete time points within the photobleaching experiment; from 0 to 1, 1 to 2, 2 to 5, 5 to 10 and 10 to 20 min.

Inter-operator reliability

Two researchers (C.K.H. and M.R.T.F.) independently analysed the image stacks from two photobleaching experiments in order to ascertain the reliability of the methods previously described. This exercise was undertaken in light of the possible variability due to manual selection of the ROI parameters, namely, size of ROI, placement of ROI within the membrane square and choice of the eight membrane squares used for analysis. Results were tested using Pearson correlation with PASW Statistics 17.0 (SPSS Inc., Chicago, IL, USA).

Results

Light exposure

The configuration of the LEDs at an angle of incidence to the sample of 30° (Fig. 1) corresponded to a radiant intensity of 0.87 per unit solid angle (Lambert's cosine law). The angle of incidence was within the angular response parameters of the cosine corrected PAR detector. The maximal radiometer reading at the sample location was 750 μmol/m^2/s, which is equivalent to 220 W/m^2 at 405 nm. Light leakage from the LEDs was minimal, being measured at 1.8 μmol/m^2/s immediately outside the obvious pool of light from a single LED. Due to the build-up of heat during operation, the light output from the LEDs dropped to 89% of their initial power after 10 min usage, after which time their output stabilized (data not shown).

Biofilm photobleaching

Photobleaching was evident in all of the samples analysed in this study: microcosm oral biofilm, *P. nigrescens* and *P. intermedia* single-species biofilms. A control experiment was designed to confirm that light was responsible for the reduction in fluorescence, in which half of the sample was shielded from

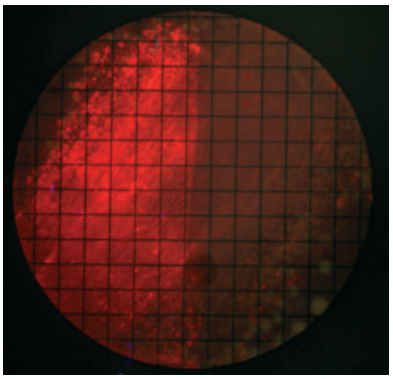

Fig. 2. Microcosm filter membrane biofilm viewed under the quantitative light-induced fluorescence digital (QLFD) lighting system. Photobleaching was demonstrated on the right-hand side of the membrane in this instance by previously covering the left-hand side of the membrane with aluminium foil whilst 405 nm light at 750 μmol/m^2/s (maximum) was incident onto the sample for 25 min. The foil was removed immediately before this image was captured (the inked squares are 4 × 4 mm).

direct illumination with aluminium foil. After 25 min, the NMPB on the exposed half dropped to 31.23 whilst the covered half was 84.73 (Fig. 2).

Figure 3 shows the results from an individual QLFD experiment, which demonstrates photobleaching as a decrease in NMPB over time. NMPB data such as these were collated to yield means along with their corresponding standard deviations (Fig. 4).

Rates of photobleaching, expressed as ΔF, were highest during the initial stages of exposure to light (i.e. the first minute). In the case of microcosm biofilms and *P. nigrescens* biofilms, photobleaching rates fell to approximately half their initial value after 10 min exposure (Fig. 5). Initial rates of photobleaching during the first minute of exposure, expressed as ΔF (arbitrary units normalized to 100 at time zero) per minute, were 19.17, 13.72 and 3.43 for *P. nigrescens* biofilm, microcosm biofilm and *P. intermedia* biofilm, respectively. Photobleaching dynamics were reproducible between replicate samples; Pearson correlation coefficient values between the four microcosm biofilm samples ranged from 0.993 to 0.997 and were significant at the 0.01 level (two-tailed).

Inter-operator reliability

Pearson correlation coefficients for the two photobleaching experiments subjected to inter-operator reliability testing were significant at the 0.01 level (two-tailed) with correlations of 0.992 and 1. The data presented herein were the first set of data that was analysed.

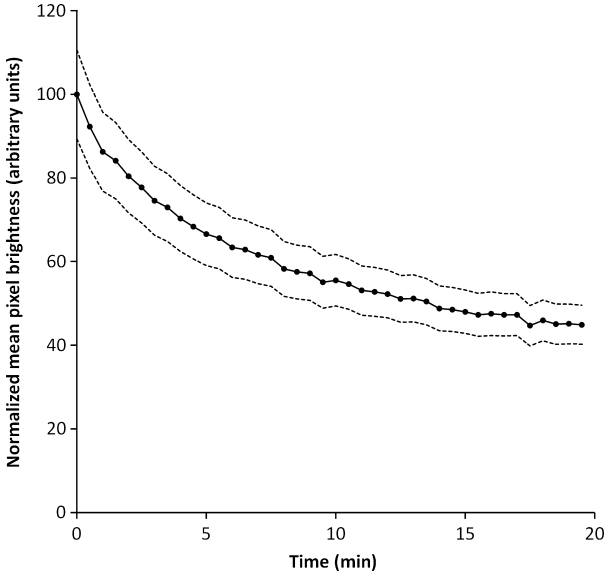

Fig. 3. A representative microcosm biofilm photobleaching experiment following illumination with the QLFD lighting system. The continuous line is the mean pixel brightness from adjacent regions of interest within the sample (n = 8); the dotted lines show standard deviations.

Discussion

Light exposure

A PAR detector was chosen to measure the light irradiance from the custom rig because photobleaching is dependent on the amount of light energy incident per unit surface area and not the power output of the LEDs *per se* (22). The camera/image analysis method of quantifying pixel brightness proved far more sensitive to subtle changes in ambient lighting conditions than the results from the PAR detector would have suggested. The data collected from the automated image sequencer yielded fewer perturbations in the fluorescence curve than when captured manually during preliminary experiments. This suggested that variation in lighting from the laptop screen, reflected off the white laboratory coat worn by the operator, was detectable in the analysed images. The inter-operator reliability data suggests that the image analysis methods employed were robust and reproducible.

Whilst every effort was made to focus the light onto the centre of the filter membrane, an *ad hoc* observation made using the PAR revealed that a single representative attempt to place the detector in the 'bright centre of the light beams' by the unaided eye yielded only 73% of the maximal irradiance obtainable by scrutinizing the meter readings. The difference between these two positions was of the order of 10 mm. Although the foci of the LEDs were generally convergent onto the sample, it is unclear how the extent of photobleaching relates to specific positions within the pool of light incident on the sample. For example, an area with less light incident upon it will fluoresce less and will likewise have a lower rate of photobleaching (23). The net result of this would be differential rates of photobleaching across a (large) sample, and a hypothetical example of this effect is demonstrated in Fig. 6. Performing image analysis on adjacent sites on the biofilm membrane will help

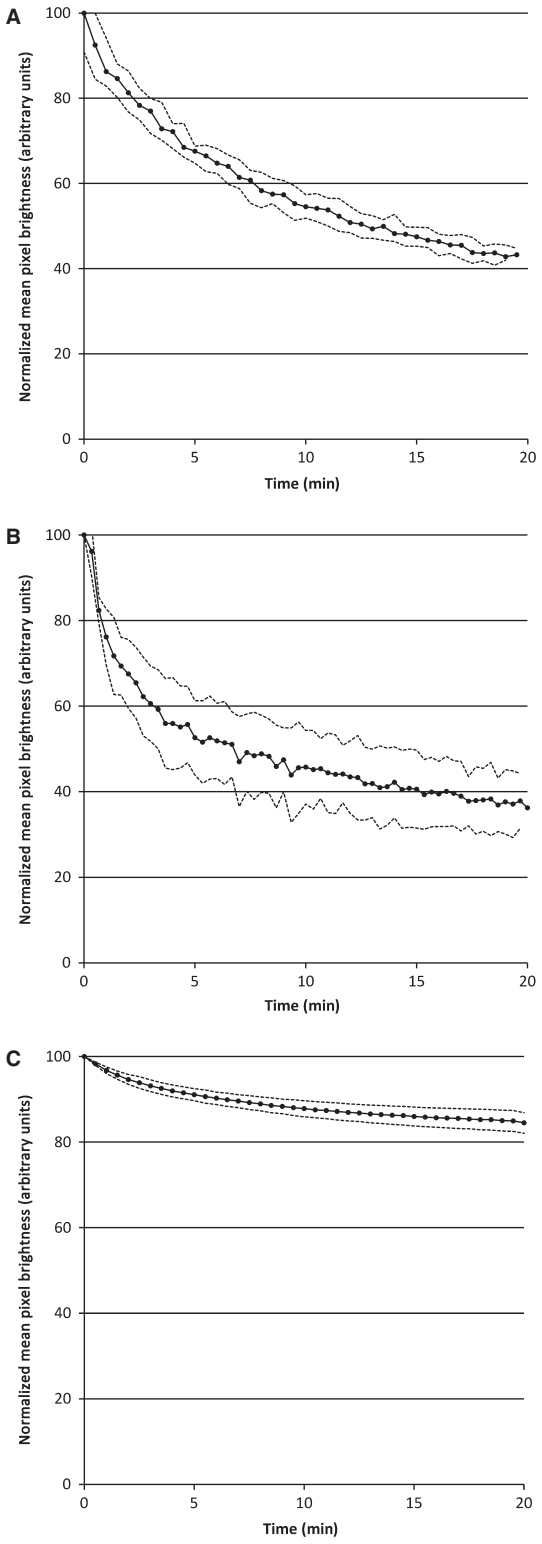

Fig. 4. Mean red fluorescence observed in microcosm ($n = 4$; A), *P. nigrescens* ($n = 2$; B) and *P. intermedia* ($n = 2$; C) filter membrane biofilms viewed under QLFD lighting. The continuous lines represent the mean values, with the dotted lines showing standard deviations.

to minimize the effects of heterogeneous lighting. Another confounding factor that should be considered is the photo-shielding effect (24), which occurs when a relatively high concentration of fluorophore absorbs excitation photons, which in turn reduces the number of photons able to penetrate into deeper layers of the sample. 'Iron porphyrin' can account for up to 50% of the dry weight of the biomass of *Bacteroides* (many of which have been reclassified as *Prevotella* spp.) when growing on blood agar (25). Photo-shielding could reduce the observed effects of photobleaching due to decreased excitation within the sample as a whole; in other words, there may not be a direct relationship between fluorescence intensity/photobleaching and net porphyrin concentration within a heterogeneous, three-dimensional microbial biofilm.

Biofilm photobleaching

Rates of photobleaching decreased during exposure to QLFD light for 20 min, after which time there was very little further reduction in observed fluorescence. It is unlikely that imaging (exposure) times beyond this would be representative of image capture *in vivo*. A reduction in mean pixel brightness of approximately 14% after 1 minillumination with QLFD represents an unacceptable inaccuracy for the quantitative analysis of the red fluorescence of dental plaque. Casual viewing and manipulation of a sample or patient under the 405 nm lighting in order to correct the focus, determine other camera settings and image capture will inevitably cause photobleaching. In order to minimize this effect, samples should be positioned and focused under normal, white-light conditions. It is, however, an unavoidable fact that in order to observe fluorescence, one must perturb fluorescence.

The rates of ΔF observed suggest that this effect was immediate and replicated the photobleaching kinetics of protoporphyrin IX previously observed in PLC hepatoma cells at 405 nm (26). In the present study, ΔF values were grouped to yield average values for all data points within discrete time bands (0–1, 1–2, 2–5, 5–10 and 10–20 min) to obviate the confounding effects of individual data points with a positive ΔF value amongst predominantly negative ΔF (i.e. fluorescence decreasing) values.

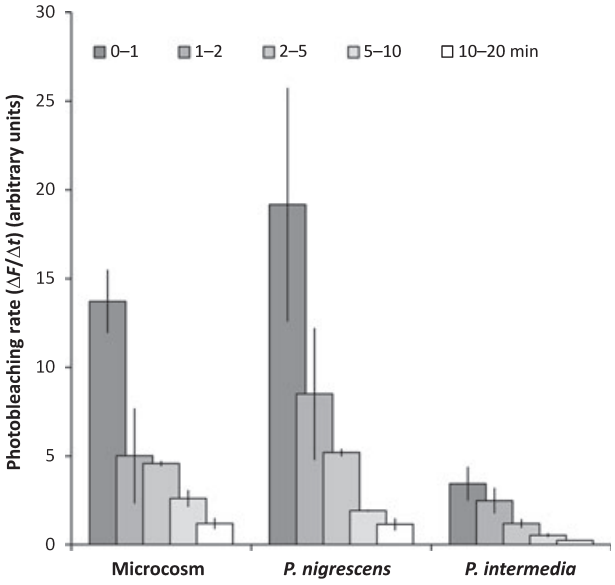

Fig. 5. Rates of photobleaching shown as the decrease in fluorescence (ΔF) with time (Δt) within a range of time points: 0–1, 1–2, 2–5, 5–10 and 10–20 min. These data correspond to Fig. 4. Error bars indicate standard deviations.

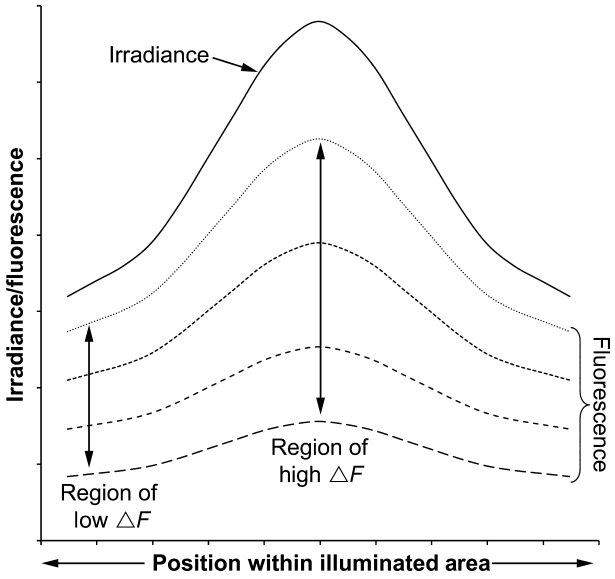

Fig. 6. A theoretical model showing differential rates of photobleaching across a sample illuminated with the custom-made lighting rig. Heterogeneous irradiance of the sample is represented by the continuous line, whereas the resulting fluorescence values are shown by the dotted lines at four time points. Fluorescence decreases over time, and the rate of photobleaching is directly proportional to the incident irradiation.

During a longitudinal study, a system whereby the LEDs are only illuminated during imaging should be employed. This will also maximize the power output of the LEDs, as they emit more light when they are at ambient (room) temperature as opposed to once they have warmed to their operating temperature. Using the PAR detector it was determined that the irradiance supplied by the lighting rig did not decrease due to heating effects when operated for 5 s out of every minute; likewise, lighting for 5 s out of every 30 s only reduced light output to 99.45% (data not shown).

The differential fluorescence of oral anaerobic bacteria under ultraviolet light has been suggested as a tool for their rapid identification. The fluorescence previously observed in strains of *Bacteridoes* (now reclassified as *Prevotella* spp. and *P. gingivalis*) encompasses a colour range that has been described as red, yellow, red-orange, brilliant red, pink-orange, orange, yellow-orange and red-brown (27). These colours also changed with age of the culture and are almost certainly a manifestation of the sequential metabolism of porphyrins (28). No fluorescence was observed in *P. gingivalis* at any time, including when emulsified in methanol; a technique that can reveal fluorescence in older cultures which have lost this capacity (2). The inability of *P. gingivalis* to fluoresce is probably due to the deposition of haem as an μ-oxo dimer on the cell surface, as opposed to the monomeric form in *Prevotella* (6,7). It was observed in preliminary experiments that the fluorescence of *P. intermedia* was greatly diminished when incubated for 7 d, hence the use of younger (5 d) cultures.

An additional experiment was conducted to see whether it was possible to use a biofilm-laden filter membrane as a rudimentary photographic plate to create a recognizable image. An acetate mask depicting the University of Liverpool logo was placed in front of a microcosm biofilm and exposed to QLFD light. After 16 min, the mask was removed to reveal a photobleached logo on the membrane (see figure S1 and figure S2).

Fluorescence imaging has the potential to be a useful tool for quantifying dental plaque in the research environment, both in terms of the amount of fluorescent material and the 'quality' of its fluorescent properties in terms of red and green fluorescence (29). The methodology described herein for measuring photobleaching of red fluorescence in microbial biofilms appears to be robust and reproducible. However, the destruction of the endogenous fluorophores within dental plaque by photobleaching phenomena, when viewed with QLFD or

similar technologies, needs to be considered and steps taken to curtail this effect in both the research and clinical environments, such as improving camera sensitivity (i.e. low shutter speeds, low apertures and high ISO settings), filter characteristics and keeping irradiance to a minimum. The reported studies do not imply that this technique has clinical applicability, but provide proof of principle data. Issues such as biofilm thickness and degree of pigmentation may influence the penetration of both the excitation and emitted fluorescent light and therefore the rate of photobleaching *in vivo*. Further research is required to determine the effects of photobleaching on plaque fluorescence.

Acknowledgements

This work was undertaken as a final year research project by M.R.T.F. and was funded internally by the University of Liverpool, School of Dental Sciences and Department of Human Anatomy and Cell Biology.

Supporting information

Additional Supporting Information may be found in the online version of this article:

Figure S1. Microcosm filter membrane biofilm masked by an acetate containing the University of Liverpool's crest.

Figure S2. Microcosm filter membrane biofilm viewed under QLFD lighting conditions to light to reveal a recognisable, photobleached image.

Please note: Wiley-Blackwell are not responsible for the content or functionality of any supporting materials supplied by the authors. Any queries (other than missing material) should be directed to the corresponding author for the article.

References

1. McGinley KJ, Webster GF, Leyden JJ. Facial follicular porphyrin fluorescence: correlation with age and density of *Propionibacterium acnes*. *Br J Dermatol* 1980;**102:**437–441.
2. Myers MB, Cherry G, Bornside BB, Bornside GH. Ultaviolet red fluorescence of *Bacteroides melaninogenicus*. *Appl Microbiol* 1969;**17:**760–762.
3. Chow AW, Patten V, Guze LB. Rapid screening of *Veillonella* by ultraviolet fluorescence. *J Clin Microbiol* 1975;**2:**546–548.
4. Lennon AM, Buchalla W, Brune L, Zimmermann O, Gross U, Attin T. The ability of selected oral microorganisms to emit red fluorescence. *Caries Res* 2006;**40:**2–5.
5. Coulthwaite L, Pretty IA, Smith PW, Higham SM, Verran J. The microbiological origin of fluorescence observed in plaque on dentures during QLF analysis. *Caries Res* 2006;**40:**112–116.
6. Smalley JW, Birss AJ, Silver J. The periodontal pathogen *Porphyromonas gingivalis* harnesses the chemistry of the mu-oxo bishaem of iron protoporphyrin IX to protect against hydrogen peroxide. *FEMS Microbiol Lett* 2000;**183:**159–164.
7. Smalley JW, Silver J, Birss AJ, Withnall R, Titler PJ. The haem pigment of the oral anaerobes *Prevotella nigrescens* and *Prevotella intermedia* is composed of iron(III) protoporphyrin IX in the monomeric form. *Microbiology* 2003;**149:**1711–1718.
8. Shah HN, Collins DM. *Prevotella*, a new genus to include *Bacteroides melaninogenicus* and related species formerly classified in the genus *Bacteroides*. *Int J Syst Bacteriol* 1990;**40:**205–208.
9. Lin DL, He LF, Li YQ. Rapid and simultaneous determination of coproporphyrin and protoporphyrin in feces by derivative matrix isopotential synchronous fluorescence spectrometry. *Clin Chem* 2004;**50:**1797–1803.
10. Stokes GG. On the change of refrangibility of light. *Philos Trans R Soc London* 1852;**142:**463–562.
11. Tong-Sheng CS-Q Z, Wei Z, Qing-Ming L. A quantitative theory model of a photobleaching mechanism. *Chin Phys Lett* 2003;**20:**1940–1943.
12. Song L, Varma CA, Verhoeven JW, Tanke HJ. Influence of the triplet excited state on the photobleaching kinetics of fluorescein in microscopy. *Biophys J* 1996;**70:**2959–2968.
13. Soukos NS, Som S, Abernethy AD *et al*. Phototargeting oral black-pigmented bacteria. *Antimicrob Agents Chemother* 2005;**49:**1391–1396.
14. Wilson M. Lethal photosensitisation of oral bacteria and its potential application in the photodynamic therapy of oral infections. *Photochem Photobiol Sci* 2004;**3:**412–418.
15. Koster M, Frahm T, Hauser H. Nucleocytoplasmic shuttling revealed by FRAP and FLIP technologies. *Curr Opin Biotechnol* 2005;**16:**28–34.
16. Bryers JD, Drummond F. Local macromolecule diffusion coefficients in structurally non-uniform bacterial biofilms using fluorescence recovery after photobleaching (FRAP). *Biotechnol Bioeng* 1998;**60:**462–473.
17. Hope CK, Wilson M. Induction of lethal photosensitization in biofilms using a confocal scanning laser as the excitation source. *J Antimicrob Chemother* 2006;**57:**1227–1230.
18. de Josselin de JE, Sundstrom F, Westerling H, Tranaeus S, ten Bosch JJ, ngmar-Mansson B. A new method for in vivo quantification of changes in initial enamel caries with laser fluorescence. *Caries Res* 1995;**29:**2–7.
19. Gmur R, Giertsen E, van dV, de Josselin de JE, Ten Cate JM, Guggenheim B. In vitro quantitative light-induced fluorescence to measure changes in enamel mineralization. *ClinOral Investig* 2006;**10**(3)**:**187–195.
20. Ando M, Hall AF, Eckert GJ, Schemehorn BR, Analoui M, Stookey GK. Relative ability of laser fluorescence techniques to quantitate early mineral loss in vitro. *Caries Res* 1997;**31:**125–131.
21. Coulthwaite L, Pretty IA, Smith PW, Higham SM, Verran J. QLF is not readily suitable for in vivo denture plaque assessment. *J Dent* 2009;**37:**898–901.
22. McCree KJ. Significance of enhancement for calculations based on the action spectrum for photosynthesis. *Plant Physiol* 1972;**49:**704–706.
23. Patterson GH, Piston DW. Photobleaching in two-photon excitation microscopy. *Biophys J* 2000;**78:**2159–2162.
24. Herzog M, Moser J, Wagner B, Broecker J. Shielding effects and hypoxia in photodynamic therapy. *Int J Oral Maxillofac Surg* 1994;**23:**406–408.
25. Rizza V, Sinclair PR, White DC, Cuorant PR. Electron transport system of the protoheme-requiring anaerobe *Bacteroides melaninogenicus*. *J Bacteriol* 1968;**96:**665–671.
26. Lu S, Chen JY, Zhang Y, Ma J, Wang PN, Peng Q. Fluorescence detection of protoporphyrin IX in living cells: a comparative study on single- and two-photon excitation. *J Biomed Opt* 2008;**13:**024014.
27. Slots J, Reynolds HS. Long-wave UV light fluorescence for identification of black-pigmented *Bacteroides* spp. *J Clin Microbiol* 1982;**16:**1148–1151.
28. Shah HN, Bonnett R, Mateen B, Williams RA. The porphyrin pigmentation of subspecies of *Bacteroides melaninogenicus*. *Biochem J* 1979;**180:**45–50.
29. Pretty IA, Edgar WM, Smith PW, Higham SM. Quantification of dental plaque in the research environment. *J Dent* 2005;**33:**193–207.